Journal of Sound and Vibration (1998) **215**(2), 231–250
Article No. sv981589

ASYMMETRIC VIBRATIONS AND ELASTIC STABILITY OF POLAR ORTHOTROPIC CIRCULAR PLATES OF LINEARLY VARYING PROFILE

U. S. Gupta and A. H. Ansari
Department of Mathematics, University of Roorkee, Roorkee 247 667, *India*

(*Received* 9 *October* 1997, *and in final form* 5 *February* 1998)

Asymmetric vibration of polar orthotropic circular plates of linearly varying thickness subjected to hydrostatic in-plane force are discussed on the basis of classical plate theory. An approximate solution of the problem has been obtained by the Ritz method, which employs functions based upon the static deflection of polar orthotropic plates. This method has a faster rate of convergence as compared to the polynomial co-ordinate functions. Frequency parameters of the plate with elastically restrained edge conditions are presented for the first three modes of vibrations for various values of taper parameter, rigidity ratio, flexibility parameter and buckling load parameter. The critical buckling loads for elastically restrained edge conditions have been obtained. A comparison of results with those available in the literature shows an excellent agreement.

1. INTRODUCTION

The development of fibre reinforced composite materials and its increasing use in the fabrication of components used in aerospace, ocean engineering, electronic equipment, etc. has necessitated the study of dynamic response of such plates. These materials, besides being light in weight, possess specific stiffness and strength. The additional weight saving can be done by considering thickness variation. Orthotropic plates have been extensively studied by various researchers such as Laura *et al*. [1, 2], Gorman [3], Gunaratnam and Bhattacharya [4], Gupta *et al*. [5–8], Vol'mir [9], Pardoen [10], Bhushan *et al*. [11, 12], etc., to mention a few. When the structural components are used in operation, they are often subjected to compressive or tensile loads. This has led to the study of buckling of orthotropic plates of variable profile.

A broad survey of literature has been carried out in this context [2, 4–6, 8–18]. An analytical solution for axisymmetric buckling of uniform orthotropic circular plate was given by Patel *et al*. [13]. In the case of axisymmetric vibrations of circular plates of variable thickness, different researchers have used different numerical techniques such as quintic splines technique [6], Chebyshev polynomial technique [7], finite element method [10–12], finite difference method [14], Frobenius method [15], and Ritz method [8, 19, 20] as no closed form solution is possible. Bhushan *et al*. [11] used the finite element technique to obtain the axisymmetric buckling of an orthotropic circular plate of linearly varying thickness. This work has been further extended by Bhushan to study the axisymmetric buckling of linearly as well as parabolically varying thickness plates [12].

A number of workers such as Kim and Dickinson [21], Laura *et al*. [19, 20, 22], Narita and Leissa [23], Irie *et al*. [24], Azimi [25, 26] have analyzed the dynamic response of uniform circular plates with restrained elastic edge conditions. Gupta *et al*. [8] studied the

0022–460X/98/320231 + 20 $30.00/0

axisymmetric vibrations and buckling of polar orthotropic circular plates of variable thickness with elastically restrained edge. In a recent paper, Laura *et al*. [19] analyzed the buckling and vibration of an isotropic non-uniform circular plate with restrained elastic edge where the radial stress distribution valid for uniform thickness plates was employed. This leads to approximate buckling load estimation.

The present work is concerned with the asymmetric buckling and vibrations of polar orthotropic circular plates of linearly varying profile with restrained elastic edge. An approximate solution has been obtained by the Ritz method using approximating functions based on the static deflection given by Lekhnitskii [27]. This type of choice of function has a faster rate of convergence as compared to polynomial co-ordinate functions used in references [8, 19, 20]. The stress resultant is obtained by solving the stress equilibrium equation by using Frobenius method [12].

2. ANALYSIS

Consider a thin circular plate of radius a, variable thickness $h = h(r)$ elastically restrained against rotation by springs of stiffness k_ϕ and subjected to hydrostatic in-plane force N at the periphery. Let (r, θ) be the polar co-ordinates of any point on the neutral surface of the circular plate shown in Figure 1.

The maximum kinetic energy of the plate is given by

$$T = \tfrac{1}{2}\rho\omega^2 \int_0^a \int_0^{2\pi} hW^2 r \,\mathrm{d}\theta\,\mathrm{d}r, \tag{1}$$

where W is the transverse deflection, ρ the mass density, and ω the frequency in rad/s.

The maximum strain energy of the plate is given by

$$\begin{aligned} U = \tfrac{1}{2}\int_0^a \int_0^{2\pi} \Bigg\{ & D_r\left\{\left(\frac{\partial^2 W}{\partial r^2}\right)^2 + 2\nu_\theta \frac{\partial^2 W}{\partial r^2}\left(\frac{1}{r}\frac{\partial W}{\partial r} + \frac{1}{r^2}\frac{\partial^2 W}{\partial \theta^2}\right)\right\} + D_\theta\left(\frac{1}{r}\frac{\partial W}{\partial r} + \frac{1}{r^2}\frac{\partial^2 W}{\partial \theta^2}\right)^2 \\ & + 4D_{r\theta}\left\{\frac{\partial}{\partial r}\left(\frac{1}{r}\frac{\partial W}{\partial \theta}\right)\right\}^2 + N_r\left(\frac{\partial W}{\partial r}\right)^2 + N_\theta\left(\frac{1}{r}\frac{\partial W}{\partial \theta}\right)^2\Bigg\} r\,\mathrm{d}\theta\,\mathrm{d}r \\ & + \tfrac{1}{2}ak_\phi \int_0^{2\pi}\left(\frac{\partial W(a,\theta)}{\partial r}\right)^2 \mathrm{d}\theta, \end{aligned} \tag{2}$$

where N_r and N_θ are the stress resultants in the r and the θ directions, respectively, and

$$D_r = \frac{E_r h^3}{12(1-\nu_r\nu_\theta)}, \qquad D_\theta = \frac{E_\theta h^3}{12(1-\nu_r\nu_\theta)}, \qquad D_{r\theta} = \frac{G_{r\theta}h^3}{12}$$

and $1/k_\phi$ is the flexibility of the rotational spring.

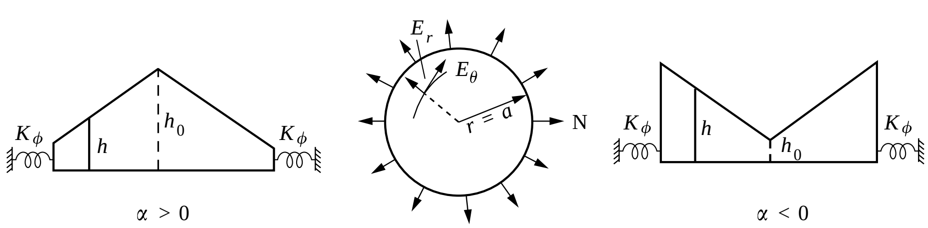

Figure 1. Circular plate.

The Ritz method requires that the functional

$$J(W) = U - T = \tfrac{1}{2}\int_0^a \int_0^{2\pi} \left\{ D_r\left\{\left(\frac{\partial^2 W}{\partial r^2}\right)^2 + 2\nu_\theta \frac{\partial^2 W}{\partial r^2}\left(\frac{1}{r}\frac{\partial W}{\partial r} + \frac{1}{r^2}\frac{\partial^2 W}{\partial \theta^2}\right)\right\}\right.$$

$$+ D_\theta\left(\frac{1}{r}\frac{\partial W}{\partial r} + \frac{1}{r^2}\frac{\partial^2 W}{\partial \theta^2}\right)^2 + 4D_{r\theta}\left\{\frac{\partial}{\partial r}\left(\frac{1}{r}\frac{\partial W}{\partial \theta}\right)\right\}^2 + N_r\left(\frac{\partial W}{\partial r}\right)^2$$

$$\left. + N_\theta\left(\frac{1}{r}\frac{\partial W}{\partial \theta}\right)^2\right\} r\,\mathrm{d}\theta\,\mathrm{d}r + \tfrac{1}{2}ak_\phi \int_0^{2\pi}\left(\frac{\partial W(a,\theta)}{\partial r}\right)^2 \mathrm{d}\theta,$$

$$- \tfrac{1}{2}\rho\omega^2 \int_0^a \int_0^{2\pi} hW^2 r\,\mathrm{d}\theta\,\mathrm{d}r \tag{3}$$

be minimized.

The deflection function is approximated as

$$\bar{\mathrm{W}} = \mathbf{W}(R)\cos n\theta = \cos n\theta \sum_{i=0}^{M} A_i \Phi_i, \tag{4}$$

where A_i are unknown constants and

$$\Phi_i = (1 + \beta_i R^4 + \delta_i R^{1+p})R^{2i+n}, \tag{5}$$

where $R = r/a$, $\bar{W} = W/a$, $p^2 = E_\theta/E_r$, n is any non-negative integer, and constants β_i and δ_i are to be determined from the boundary conditions. The choice of the functions are based upon the static deflection of polar orthotropic circular plates [27] (p. 370), [28] (p. 336). Using the non-dimensional variables and relation (4), the functional (3) becomes

$$J(\mathbf{W}) = \frac{\pi a^2}{2}\int_0^1 \left\{ D_r\left\{\left(\frac{\partial^2 \mathbf{W}}{\partial R^2}\right)^2 + 2\nu_\theta \frac{\partial^2 \mathbf{W}}{\partial R^2}\left(\frac{1}{R}\frac{\partial \mathbf{W}}{\partial R} - \frac{n^2\mathbf{W}}{R^2}\right)\right\} + D_\theta\left(\frac{1}{R}\frac{\partial \mathbf{W}}{\partial R} - \frac{n^2\mathbf{W}}{R^2}\right)^2\right.$$

$$\left. + 4n^2 D_{r\theta}\left(\frac{1}{R}\frac{\partial \mathbf{W}}{\partial R} - \frac{1}{R^2}\mathbf{W}\right)^2 + N_r\left(\frac{\partial \mathbf{W}}{\partial R}\right)^2 + n^2 N_\theta\left(\frac{\mathbf{W}}{R}\right)^2\right\} R\,\mathrm{d}R$$

$$+ \tfrac{1}{2}ak_\phi \int_0^{2\pi}\left(\frac{\partial \mathbf{W}(1,\theta)}{\partial R}\right)^2 \mathrm{d}\theta, \qquad -\frac{\pi}{2}a^4\rho\omega^2 \int_0^1 h\mathbf{W}^2 R\,\mathrm{d}R. \tag{6}$$

The stress equilibrium equation for N_r together with the compatibility equation [29] for a linearly varying thickness $h = h_0(1 - \alpha R)$ gives

$$R^2\frac{\mathrm{d}^2 N_r}{\mathrm{d}R^2} + \frac{(3 - 2\alpha R)}{(1 - \alpha R)} R\frac{\mathrm{d}N_r}{\mathrm{d}R} + \left((1 - p^2) - \frac{(1 - \nu_\theta)\alpha R}{1 - \alpha R}\right)N_r = 0. \tag{7}$$

The solution of N_r obtained by Frobenius method [11] is given by

$$N_r = \frac{N}{\left\{1 + \sum_{i=1}^{\infty} C_i\right\}} R^\lambda \left\{1 + \sum_{i=1}^{\infty} C_i R^i\right\}, \tag{8}$$

where

$$\lambda = 1 - p, \qquad C_1 = \frac{\lambda(\lambda+2) + 1 - p^2 - (\lambda + 1 - \nu_\theta)}{(\lambda+2)^2 - p^2}\,\alpha,$$

$$C_i = \frac{(\lambda + i - 1)(\lambda + i + 1) + 1 - p^2 - (\lambda + i - \nu_\theta)}{(\lambda + i + 1)^2 - p^2}\,\alpha C_{i-1}, \qquad i = 2, 3, \ldots, \infty.$$

The minimization of the functional $J(\mathbf{W})$ given by equation (6) requires

$$\frac{\partial}{\partial A_i} J(\mathbf{W}) = 0, \qquad i = 0, 1, \ldots, M, \tag{9}$$

which leads to a system of homogeneous equations in A_i, $i = 0, 1, M$ and its non-trivial solution leads to the frequency equation

$$|A - \Omega^2 B| = 0, \tag{10}$$

where $A = [a_{ij}]$ and $B = [b_{ij}]$ are square matrices of order M and

$$a_{ij} = \int_0^1 (1 - \alpha R)^3 \left\{ \Phi_i'' \Phi_j'' + 2\nu_\theta \Phi_i'' \left(\frac{\Phi_j'}{R} - \frac{n^2}{R^2}\Phi_j \right) + p^2 \left(\frac{\Phi_i'}{R} - \frac{n^2}{R^2}\Phi_i \right)\left(\frac{\Phi_j'}{R} - \frac{n^2}{R^2}\Phi_j \right) \right.$$
$$\left. + n^2 D_{k0} \left(\frac{\Phi_i'}{R} - \frac{1}{R^2}\Phi_i \right)\left(\frac{\Phi_j'}{R} - \frac{1}{R^2}\Phi_j \right) + \frac{N_r}{D_{r0}} \Phi_i' \Phi_j' + n^2 \frac{N_\theta}{D_{r0}} \Phi_{i-1}\Phi_{j-1} \right\} R \, \mathrm{d}R$$
$$+ K_\phi \Phi_i'(1) \Phi_j'(1) \tag{11}$$

and

$$b_{ij} = \int_0^1 (1 - \alpha R) \Phi_i \Phi_j R \, \mathrm{d}R, \tag{12}$$

where

$$K_\phi = \frac{a k_\phi}{D_{r0}}, \quad D_{k0} = 4\frac{D_{r\theta}}{D_{r0}}, \quad \Omega^2 = \frac{h_0 a^4 \rho \omega^2}{D_{r0}} \quad \text{and} \quad \bar{N} = \frac{N a^2}{D_{r0}}.$$

As each function Φ_i has to satisfy the boundary conditions [31] (p. 14), one has

$$K_\phi = \frac{\mathrm{d}\mathbf{W}(1)}{\mathrm{d}R} = -(1-\alpha)^3 \left[\frac{\mathrm{d}^2\mathbf{W}}{\mathrm{d}R^2} + \nu_\theta \left(\frac{1}{R}\frac{\mathrm{d}\mathbf{W}}{\mathrm{d}R} - \frac{n^2 \mathbf{W}}{R^2} \right) \right]_{R=1}, \tag{13}$$

$$\mathbf{W}(1) = 0. \tag{14}$$

The unknown constants β_i and δ_i are determined using these boundary conditions.

3. NUMERICAL RESULTS

The frequency equation (10) has been solved for various values of plate parameters such as taper parameter α, rigidity ratio E_θ/E_r $(=p^2)$, flexibility parameter K_ϕ and the buckling load parameter $\bar{N}$ $(=Na^2/D_{r0})$. The numerical results have been calculated for

$\alpha(=-0{\cdot}5(0{\cdot}2)0{\cdot}5;\ 0{\cdot}0)$, E_θ/E_r $(=0{\cdot}75,\ 1{\cdot}0,\ 2{\cdot}0,\ 5{\cdot}0,\ 10{\cdot}0)$, $K_\phi(=0,\ 10,\ 10^2,\ 10^{20}\cong\infty)$ and $\bar{N}(=0,\ \pm 10,\ \pm 20)$ for the first three modes of asymmetric vibrations i.e., $n=0$, 1, 2. The Poisson ratio ν_θ and shear rigidity modulus $D_{r\theta}/D_{r0}$ have been taken as 0·3 and 0·35, respectively. Special cases of classical boundary conditions i.e., simply-supported and clamped, have been considered by taking appropriate values of flexibility parameters. The critical buckling parameter N_{cr} has been obtained for $E_\theta/E_r(=0{\cdot}75,\ 1{\cdot}0,\ 10{\cdot}0)$ in fundamental mode for different values of K_ϕ, taper parameter α and nodal diameter n.

4. DISCUSSION

The results are presented in Tables (1–12) and Figures (2–13). Tables (1–3) show the effect of the rigidity ratio E_θ/E_r and that of taper parameter α on the critical buckling load parameter N_{cr} for different values of rotational flexibility parameter $K_\phi(=0,\ 10,\ 10^2,\ 10^{20}\cong\infty)$, when the plate is vibrating in fundamental mode with 0, 1 and 2 nodal diameters. The critical buckling load parameter N_{cr} is found to increase with the increasing values of rigidity ratio E_θ/E_r. It is also found to increase with increasing values of flexibility parameter K_ϕ and the nodal diameter n. Furthermore, the critical buckling load parameter

Table 1

Critical buckling load parameter N_{cr} for orthotropic circular plate of variable thickness in fundamental mode for $\nu_\theta=0{\cdot}3$ and $n=0$

K_ϕ	α/p^2	0·75	1·0	2·0	5·0	10·0
	−0·5	6·5411	8·5033	16·3063	39·6451	78·5908
	−0·3	5·1254	6·5448	12·0768	28·2072	54·6444
	−0·1	3·9254	4·9070	8·6435	19·2026	36·1223
0	0·0	3·3988	4·1978	7·1980	15·5209	28·6770
	0·1	2·9174	3·5561	5·9186	12·3371	22·3259
	0·3	2·0783	2·4583	3·8144	7·3162	12·5571
	0·5	1·3836	1·5784	2·2425	3·8461	6·1179
	−0·5	17·5025	21·3108	35·1782	71·4925	125·7812
	−0·3	14·5680	17·6255	28·6321	56·8441	97·9516
	−0·1	11·6329	13·9679	22·3114	43·4151	73·6467
10	0·0	10·1840	12·1725	19·2479	37·0613	62·4710
	0·1	8·7673	10·4222	16·2808	30·9591	51·8510
	0·3	6·0993	7·1460	10·7941	19·7809	32·4976
	0·5	3·7726	4·3256	6·2024	10·6565	16·8125
	−0·5	24·5804	30·5336	53·2002	116·6735	216·0948
	−0·3	18·9535	23·3147	39·7230	85·0705	155·8026
	−0·1	14·0743	17·1122	28·3577	58·8289	105·8356
10^2	0·0	11·9182	14·3922	23·4638	47·7311	84·8533
	0·1	9·9497	11·9243	19·0868	37·9615	66·5234
	0·3	6·5685	7·7305	11·8358	22·2464	37·5361
	0·5	3·9085	4·4904	6·4767	11·2488	17·9504
	−0·5	25·6908	32·0360	56·5170	127·1290	242·3347
	−0·3	19·5766	24·1521	41·4971	90·3931	168·7801
	−0·1	14·3916	17·5375	29·2179	61·2621	90·9746
10^{20}	0·0	12·1428	14·6820	24·0350	49·2949	83·5167
	0·1	10·0890	12·1143	19·4512	38·9227	68·6733
	0·3	6·6247	7·8007	11·9624	22·5560	38·1817
	0·5	3·9240	4·5095	6·5083	11·3186	18·0847

TABLE 2

Critical buckling load parameter N_{cr} for orthotropic circular plate of variable thickness in fundamental mode for $\nu_\theta = 0{\cdot}3$ and $n = 1$

K_ϕ	α/p^2	0·75	1·0	2·0	5·0	10·0
	−0·5	26·1503	28·8695	38·9138	66·6294	110·6255
	−0·3	19·8092	21·6961	28·6272	47·5294	77·2012
	−0·1	14·4741	15·7121	20·2316	32·3892	51·2155
0	0·0	12·1623	13·1381	16·6884	26·1654	40·7239
	0·1	10·0761	10·8276	13·5524	20·7649	31·7460
	0·3	6·5450	6·9514	8·4137	12·2112	17·8697
	0·5	3·8097	3·9909	4·6381	6·2815	8·6625
	−0·5	36·8704	41·0104	55·8630	94·6049	152·5184
	−0·3	29·8121	32·9778	44·2814	73·4106	116·2696
	−0·1	23·3642	25·6855	33·9505	55·0787	85·8165
10	0·0	20·3373	22·2776	29·1804	46·7835	72·3157
	0·1	17·4365	19·0221	24·6587	39·0052	59·7836
	0·3	12·0470	13·0080	16·4163	25·0438	37·5085
	0·5	7·3395	7·8137	9·4871	13·6668	19·6318
	−0·5	47·2316	53·4694	76·4981	139·7511	238·7446
	−0·3	36·7496	41·2570	57·8043	102·8660	173·1482
	−0·1	27·5220	30·5976	41·8092	71·9606	118·5781
10^2	0·0	23·3882	25·8594	34·8310	58·7696	95·5469
	0·1	19·5784	21·5182	28·5296	47·0705	75·3242
	0·3	12·9374	14·0268	17·9260	28·0174	43·0645
	0·5	7·6049	8·1101	9·8992	14·4087	20·9310
	−0·5	49·3256	56·0582	81·1792	151·9579	266·8726
	−0·3	37·9516	42·7204	60·3523	109·1951	187·2921
	−0·1	28·1505	31·3498	43·0639	74·9028	124·9059
10^{20}	0·0	23·8228	26·3746	35·6702	60·6741	99·5435
	0·1	19·8677	21·8578	29·0688	48·2512	77·7376
	0·3	13·0479	14·1536	18·1160	28·4003	43·7993
	0·5	7·6360	8·1448	9·9477	14·4967	21·0864

N_{cr} is greater for the negative values of the taper parameter α than those for positive values, when all other plate parameters are kept fixed. This may be attributed to the greater thickness of the plate for negative values of α. The classical boundary conditions for simply supported (SS) and clamped (Cl) edge are obtained by taking the rotational flexibility parameter $K_\phi = 0$ and $K_\phi = 10^{20} \cong \infty$, respectively. Figures 2(a) and (b) show the plot of in-plane force parameter $\bar{N}$ versus frequency parameter Ω in the fundamental mode for $n = 0$, 1 and 2. The solid and the dashed lines respectively denote the clamped and simply supported edge conditions. The critical buckling load parameter N_{cr} for a clamped plate is always greater than that for a simply supported plate other plate parameters being fixed. It is also seen that the critical buckling load increases with the increase in nodal diameters for both the boundary conditions. Figure 3 shows the plot for N_{cr} versus taper parameter α. The critical buckling load is found to increase with the decreasing values of taper parameter α, the rate of increase in the circumferential stiffened plate $E_\theta > E_r$ is greater as compared to the radially stiffened (i.e., $E_\theta < E_r$). It is further seen that the rate of increase (when taper α decreases) is greater in the case of clamped as compared to the simply supported edge condition. Figure 4 shows the effect of rigidity ratio E_θ/E_r and taper

TABLE 3

Critical buckling load parameter N_{cr} for orthotropic circular plate of variable thickness in fundamental mode for $v_\theta = 0{\cdot}3$ and $n = 0$

K_ϕ	α/p^2	0·75	1·0	2·0	5·0	10·0
	−0·5	51·0212	56·3308	74·9526	120·1574	183·7438
	−0·3	38·2290	41·8894	54·6359	85·2514	127·9366
	−0·1	27·5622	29·9485	38·1858	57·7101	84·6271
	−0·0	22·9802	24·8557	31·2949	46·4345	67·1710
0	0·1	18·8739	20·3152	25·2321	36·6874	52·2570
	0·3	12·0114	12·7900	15·4007	21·3401	29·2609
	0·5	6·8138	7·1651	8·3097	10·8220	14·0841
	−0·5	61·2172	67·9265	91·2226	146·7796	223·0693
	−0·3	48·3027	53·2409	70·3385	110·6550	165·4272
	−0·1	37·0687	40·5830	52·6231	80·8716	118·8304
10	0·0	32·0073	34·9049	44·8331	67·9583	98·9925
	0·1	27·2649	29·6118	37·6271	56·2138	81·0875
	0·3	18·6952	20·1038	24·8733	35·8312	50·4382
	0·5	11·3704	12·0697	14·3989	19·6315	26·5344
	−0·5	73·9863	83·1660	116·0144	198·0613	315·7143
	−0·3	57·3338	63·9400	87·4235	145·5533	228·8310
	−0·1	42·7932	47·2857	63·1105	101·8401	156·9332
10^2	0·0	36·3119	39·9191	52·5514	83·2511	126·6221
	0·1	30·3601	33·1894	43·0375	66·7112	100·0173
	0·3	20·0282	21·6204	27·0705	39·8888	57·5209
	0·5	11·7771	12·5212	15·0122	20·6777	28·2507
	−0·5	77·1312	87·0289	122·7886	214·6841	351·3377
	−0·3	59·1512	66·1500	91·1682	154·3120	247·0178
	−0·1	43·7567	48·4316	64·9729	105·9623	165·1591
10^{20}	0·0	36·9771	40·7065	53·7983	85·9090	131·8527
	0·1	30·8024	33·7096	43·8407	68·4030	103·1915
	0·3	20·1881	21·8152	27·5453	40·4238	58·4961
	0·5	11·8248	12·5747	15·0812	20·8017	28·4600

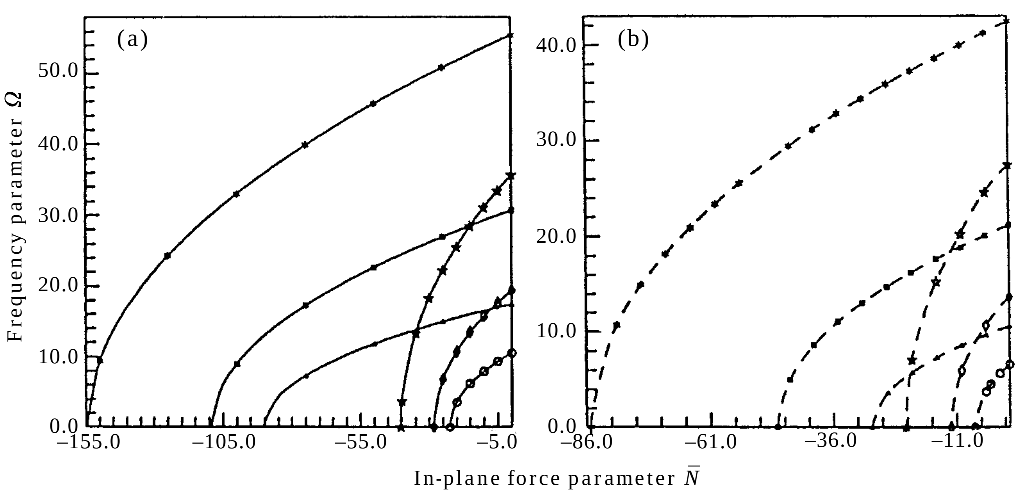

Figure 2. (a) In-plane force parameter $\bar{N}$ versus frequency parameter for Cl: ——, plate in fundamental mode for $v_\theta = 0{\cdot}3$ and $E_\theta/E_r = 5{\cdot}0$. (b) In-plane force parameter $\bar{N}$ versus frequency parameter for SS – – –, plate in fundamental mode for $v_\theta = 0{\cdot}3$ and $E_\theta/E_r = 5{\cdot}0$. ▲▲▲, $n = 0$, $\alpha = -0{\cdot}3$; ■■■, $n = 1$, $\alpha = -0{\cdot}3$; ★★★, $n = 2$, $\alpha = -0{\cdot}3$; ○○○, $n = 0$, $\alpha = 0{\cdot}3$; ◇◇◇, $n = 1$, $\alpha = 0{\cdot}3$; ☆☆☆, $n = 2$, $\alpha = 0{\cdot}30$.

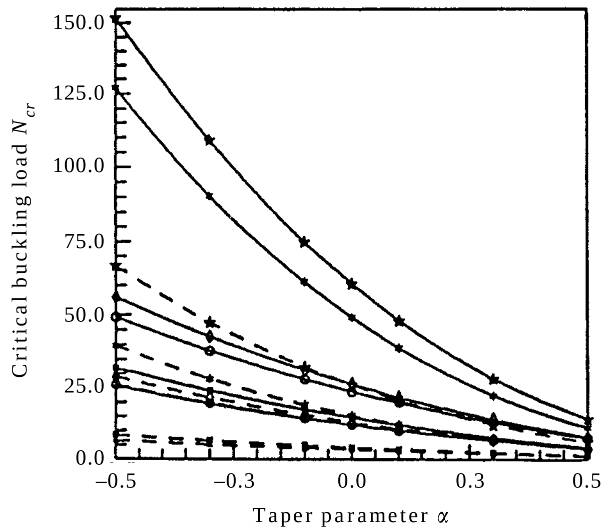

Figure 3. Effect of taper parameter on the buckling load parameter for SS (– – –) and Cl (——) LVT plates for $\nu_\theta = 0{\cdot}3$ ▲▲▲, $p = 0{\cdot}75$, $n = 0$; ■■■, $p = 1{\cdot}0$, $n = 0$; ★★★, $p = 5{\cdot}0$, $n = 0$; ○○○, $p = 0{\cdot}75$, $n = 1$; ◇◇◇, $p = 1{\cdot}0$, $n = 1$; ☆☆☆, $p = 5{\cdot}0$, $n = 1$.

α on the radial stress resultant N_r. These are plotted against the radius for different values of E_θ/E_r (=10, 1 and 0·1) and α (= +0·3, 0 and −0·3). The stress resultant remains constant for isotropic ($E_\theta/E_r = 1$) plates of uniform thickness (i.e., $\alpha = 0$). The radial stress resultant is monotonically increasing for circumferentially stiffened paltes ($E_\theta > E_r$) for radial values chosen from edge to centre. However, the behaviour is just the reverse for radially stiffened plates ($E_\theta < E_r$). It also demonstrates that the effect of taper parameter α on the stress resultant is quite appreciable. For fixed values of rigidity ratio E_θ/E_r, the stress resultant for centrally thick plates is greater as compared to centrally thin and uniform plates.

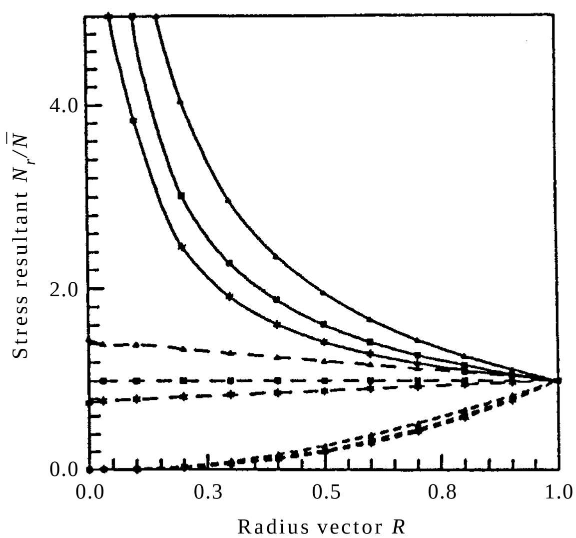

Figure 4. Radial stress resultant versus radius vector for $p = 0{\cdot}1$ (——), $p = 1{\cdot}0$ (– – –) and $p = 10$ (. . . .). ■■■, $\alpha = 0{\cdot}0$; ★★★, $\alpha = -0{\cdot}3$; ▲▲▲, $\alpha = 0{\cdot}3$.

Table 4

Values of the frequency parameter Ω of orthotropic circular plates of linearly varying thickness in fundamental mode of vibrations for $v_\theta = 0{\cdot}3$, $E_\theta/E_r = 0{\cdot}75$, $D_{k0} = 1{\cdot}4$ and $n = 0$

K_ϕ	$\bar{N}/\alpha$	−0·5	−0·3	−0·1	0·0	0·1	0·3	0·5
	−20	–	–	–	–	–	–	–
	−10	–	–	–	–	–	–	–
0	0	5·6789	5·2236	4·7694	4·5418	4·3131	3·8485	3·3621
	10	9·0229	8·9680	8·9807	9·0166	9·0750	9·2700	9·5922
	20	11·4218	11·5536	11·7696	11·9144	12·0870	12·5282	13·1236
	−20	–	–	–	–	–	–	–
	−10	6·4653	5·2922	3·3271	–	–	–	–
10	0	9·7863	9·3413	8·7516	8·3877	7·9709	6·9678	5·7402
	10	12·1846	12·0313	11·8196	11·6874	11·5378	11·2007	10·8723
	20	14·1535	14·1837	14·1943	14·1906	14·1822	14·1674	14·2130
	−20	5·8016	–	–	–	–	–	–
	−10	10·1618	8·1724	5·6564	3·9315	–	–	–
10^2	0	13·0027	11·7003	10·3264	9·6167	8·8943	7·4170	5·9030
	10	15·2397	14·2809	13·3317	12·8733	12·4338	11·6425	11·0342
	20	17·1324	16·3981	15·7045	15·3863	15·0961	14·6315	14·3902
	−20	6·6644	–	–	–	–	–	–
	−20	10·8772	8·6342	5·9547	4·1956	–	–	–
10^{20}	0	13·7233	12·1506	10·5854	9·8056	9·0276	7·4753	5·9225
	10	15·9873	14·7508	13·6038	13·0723	12·5746	11·7042	11·0547
	20	17·9118	16·8927	15·9943	15·5999	15·2484	14·6996	14·4134

Tables (4–6) and Figure 5 show the effect of in-plane force parameter $\bar{N}$ ($= -20(10)20$) for different values of rigidity ratio and flexibility parameter K_ϕ for axisymmetric vibrations (i.e., $n = 0$) of the plate vibrating in fundamental mode. It has been seen that the frequency parameter Ω gradually increases with the increase of $\bar{N}$ and also of the taper parameter

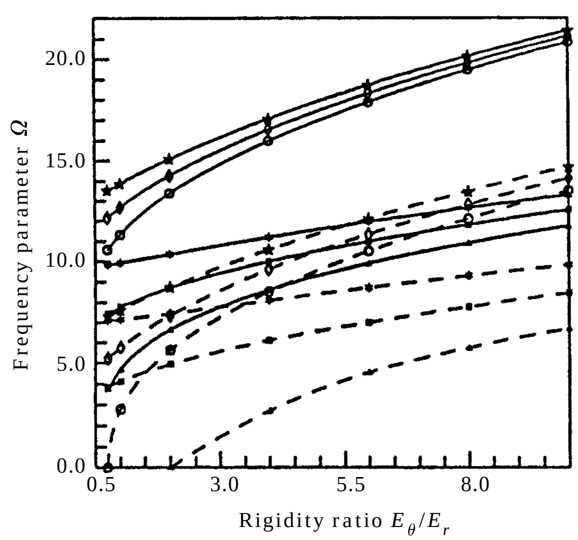

Figure 5. Frequency parameter in axisymmetric fundamental mode for SS (– – –) and Cl (——) LVT plates for $v_\theta = 0{\cdot}3$. ▲▲▲, $N = -5$, $\alpha = 0{\cdot}3$; ■■■, $N = 0$, $\alpha = 0{\cdot}3$; ★★★, $N = 5$, $\alpha = 0{\cdot}3$; ○○○, $N = -5$, $\alpha = -0{\cdot}3$; ◇◇◇, $N = 0$, $\alpha = -0{\cdot}3$; ☆☆☆, $N = 5$, $\alpha = -0{\cdot}3$.

TABLE 5

Values of the frequency parameter Ω of orthotropic circular plates of linearly varying thickness in fundamental mode of vibrations for $\nu_\theta = 0{\cdot}3$, $E_\theta/E_r = 1{\cdot}0$, $D_{k0} = 1{\cdot}4$ *and* $n = 0$

K_ϕ	$\bar{N}/\alpha$	−0·5	−0·3	−0·1	0·0	0·1	0·3	0·5
	−20	–	–	–	–	–	–	–
	−10	–	–	–	–	–	–	–
0	0	6·2928	5·7483	5·2061	4·9351	4·6637	4·1158	3·5498
	10	9·2818	9·1392	9·0729	9·0732	9·0989	9·2381	9·5181
	20	11·5192	11·5760	11·7267	11·8425	11·9889	12·3855	12·9466
	−20	2·5720	–	–	–	–	–	–
	−10	7·5176	6·4665	4·9054	3·7263	–	–	–
10	0	10·2792	9·7804	9·1407	8·7519	8·3098	7·2518	5·9608
	10	12·4215	12·1964	11·9150	11·7485	11·5653	11·1649	10·7849
	20	14·2322	14·1897	14·1318	14·0958	14·0572	13·9905	14·0016
	−20	8·1042	4·6920	–	–	–	–	–
	−10	11·2056	9·2988	7·0056	5·5919	3·7612	6·1301	–
10^2	0	13·5534	12·1950	10·7607	10·0192	9·2639	7·7176	6·1301
	10	15·5075	14·4705	13·4419	12·9443	12·4669	11·6063	10·9449
	20	17·2110	16·3982	15·6305	15·2786	14·9575	14·4432	14·1725
	−20	8·9200	5·3548	–	–	–	–	–
	−10	11·9568	9·7789	7·3013	5·8274	3·9696	–	–
10^{20}	0	14·3022	12·6631	11·0301	10·2158	9·4027	7·7783	6·1504
	10	16·2706	14·9488	13·7177	13·1455	12·6088	11·6680	10·9652
	20	17·9941	16·8925	15·9183	15·4897	15·1074	14·5095	14·1950

TABLE 6

Values of the frequency parameter Ω of orthotropic circular plates of linearly varying thickness in fundamental mode of vibrations for $\nu_\theta = 0{\cdot}3$, $E_\theta/E_r = 10{\cdot}0$, $D_{k0} = 1{\cdot}4$ *and* $n = 0$

k_ϕ	$\bar{N}/\alpha$	−0·5	−0·3	−0·1	0·0	0·1	0·3	0·5
	−20	14·0177	11·4499	8·3968	6·4302	3·4990	–	–
	−10	15·0762	12·8827	10·5378	9·2604	7·8543	3·9844	–
0	0	16·0450	14·1334	12·2320	11·2858	10·3429	8·4682	6·6083
	10	16·9410	15·2506	13·6579	12·9124	12·2112	10·9845	10·0792
	20	17·7763	16·2648	14·9010	14·2913	13·7408	12·8523	12·3010
	−20	17·4826	15·5908	13·5144	12·3430	11·0221	7·5047	–
	−10	18·2205	16·4802	14·6269	13·6178	12·5220	9·9187	6·1477
10	0	18·9209	17·3110	15·6400	14·7563	13·8241	11·7661	9·3945
	10	19·5884	18·0922	16·5741	15·7910	14·9845	13·3002	11·6074
	20	20·2267	18·8308	17·4432	16·7433	16·0373	14·6302	13·3588
	−20	21·7845	19·1181	16·1908	14·5954	12·8738	8·7283	–
	−10	22·2955	19·7623	17·0457	15·6073	14·1029	10·8048	6·5961
10^2	0	22·7924	20·3814	17·8503	16·5433	15·2112	12·4786	9·6620
	10	23·2760	20·9777	18·6115	17·4169	16·2256	13·9056	11·8123
	20	23·7474	21·5535	19·3351	18·2377	17·1644	15·1627	13·5318
	−20	23·0268	19·9228	16·6771	14·9628	13·1466	8·8777	–
	−10	23·5044	20·5367	17·5041	15·9474	14·3484	10·9214	6·6479
10^{20}	0	23·9702	21·1286	18·2850	16·8616	15·4364	12·5772	9·6949
	10	24·4251	21·7004	19·0260	17·7170	16·4349	13·9928	11·8385
	20	24·8696	22·2538	19·7320	18·5227	17·3610	15·2421	13·5546

TABLE 7

Values of the frequency parameter Ω of orthotropic circular plates of linearly varying thickness in fundamental mode of vibrations for $\nu_\theta = 0{\cdot}3$, $E_\theta/E_r = 0{\cdot}75$, $D_{k0} = 1{\cdot}4$ and $n = 1$

K_ϕ	$\bar{N}/\alpha$	−0·5	−0·3	−0·1	0·0	0·1	0·3	0·5
	−20	8·5794	–	–	–	–	–	–
	−10	13·8858	11·3101	8·0346	5·7470	–	–	–
0	0	17·6517	16·0622	14·4482	13·6291	12·7995	11·0979	9·3084
	10	20·7370	19·6936	18·7847	18·3971	18·0663	17·6245	17·5915
	20	23·4140	22·7491	22·2918	22·1618	22·1120	22·3084	23·0176
	−20	14·7331	11·7999	7·2967	–	–	–	–
	−10	18·5207	16·6887	14·4606	13·0899	11·4425	6·4039	–
10	0	21·6234	20·3941	19·0371	18·2759	17·4373	15·4606	12·9922
	10	24·3114	23·4939	22·6711	22·2422	21·7948	20·8448	19·9087
	20	26·7144	26·2103	25·7740	25·5748	25·3871	25·0677	24·9433
	−20	20·4900	16·6642	11·6001	7·9432	–	–	–
	−10	23·7975	20·9052	17·5653	15·6612	13·5264	7·8495	–
10^2	0	26·6445	24·3501	21·8730	20·5671	19·2168	16·3800	13·3429
	10	29·1750	27·3153	25·4028	24·4458	23·5027	21·7202	20·2346
	20	31·4717	29·9525	28·4580	27·7461	27·0767	25·9444	25·2764
	−20	21·9279	17·6136	12·2316	8·5199	–	–	–
	−10	25·2256	21·8213	18·1119	16·0714	13·8289	8·0229	–
10^{20}	0	28·0859	25·2701	22·4130	20·9646	19·4998	16·5060	13·3859
	10	30·6399	28·2522	25·9531	24·8506	23·7903	21·8469	20·2764
	20	32·9648	30·9115	29·0242	28·1638	27·3744	26·0765	25·3206

α. It can be further observed that for a centrally thicker plate, the frequency parameter Ω is smaller than that of a centrally thinner plate.

Tables (7–9) and Figure 6 show the frequency parameter Ω for the antisymmetric ($n = 1$) fundamental mode for different values of rigidity ratio and in-plane force parameter $\bar{N}$.

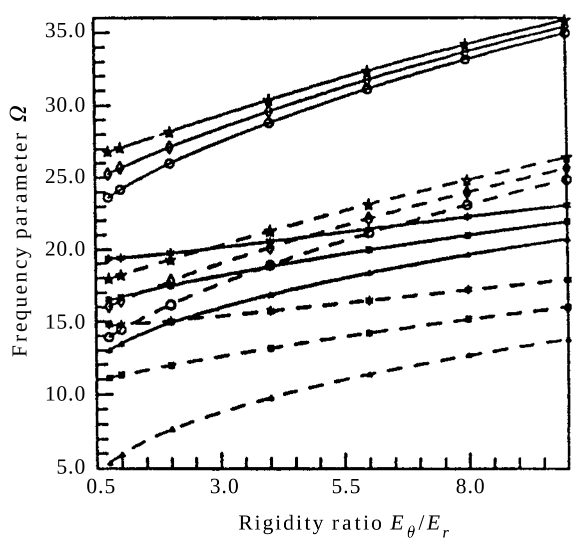

Figure 6. Frequency parameter in antisymmetric ($n = 1$) fundamental mode for SS (– – –) and Cl (——) LVT plates for $\nu_\theta = 0{\cdot}3$. Key as for Figure 5.

TABLE 8

Values of the frequency parameter Ω of orthotropic circular plates of linearly varying thickness in fundamental mode of vibrations for $\nu_\theta = 0{\cdot}3$, $E_\theta/E_r = 1{\cdot}0$, $D_{k0} = 1{\cdot}4$ and $n = 1$

K_ϕ	$\bar{N}/\alpha$	−0·5	−0·3	−0·1	0·0	0·1	0·3	0·5
	−20	10·0292	4·5941	–	–	–	–	–
	−10	14·6229	12·0623	8·8928	6·7932	3·6064	–	–
0	0	18·0815	16·4266	14·7487	13·8982	13·0377	11·2763	9·4302
	10	20·9751	19·8526	18·8669	18·4425	18·0762	17·5695	17·4825
	20	23·5135	22·7681	22·2349	22·0694	21·9861	22·1224	22·7810
	−20	15·8274	13·0703	9·1440	5·9645	–	–	–
	−10	19·1894	17·3491	15·1424	13·8020	12·2095	7·5496	–
10	0	22·0288	20·7418	19·3308	18·5438	17·6799	15·6528	13·1326
	10	24·5306	23·6377	22·7405	22·2749	21·7912	20·7711	19·7743
	20	26·7913	26·2049	25·6881	25·4497	25·2241	24·8352	24·6579
	−20	21·5985	17·9037	13·1794	10·0196	5·2211	–	–
	−10	24·5093	21·6102	18·2839	16·4016	14·3083	8·9180	–
10^2	0	27·0779	24·7269	22·1924	20·8575	19·4780	16·5828	13·4875
	10	29·3984	27·4622	25·4721	24·4765	23·4953	21·6412	20·0960
	20	31·5288	29·9253	28·3487	27·5976	26·8911	25·6944	24·9815
	−20	23·0742	18·8741	13·8055	10·5472	5·8147	–	–
	−10	25·9680	22·5470	18·8431	16·8206	14·6163	9·0860	–
10^{20}	0	28·5387	25·6595	22·7398	21·2604	19·7648	16·7104	13·5310
	10	30·8711	28·4027	26·0233	24·8814	23·7826	21·7671	20·1373
	20	33·0189	30·8796	28·9098	28·0106	27·1848	25·8238	25·0244

TABLE 9

Values of the frequency parameter Ω of orthotropic circular plates of linearly varying thickness in fundamental mode of vibrations for $\nu_\theta = 0{\cdot}3$, $E_\theta/E_r = 10{\cdot}0$, $D_{k0} = 1{\cdot}4$ and $n = 1$

K_ϕ	$\bar{N}/\alpha$	−0·5	−0·3	−0·1	0·0	0·1	0·3	0·5
	−20	26·3062	22·3172	17·8153	15·1857	12·0323	–	–
	−10	27·6255	24·0664	20·3036	18·2914	16·1331	10·8917	–
0	0	28·8702	25·6691	22·4593	20·8499	19·2365	15·9916	12·7048
	10	30·0502	27·1530	24·3769	23·0557	21·7965	19·5420	17·8331
	20	31·1735	28·5386	26·1137	25·0111	24·0040	22·3635	21·3900
	−20	30·2555	27·0917	23·6895	21·8090	19·7221	14·3592	–
	−10	31·3036	28·3772	25·3206	23·6855	21·9300	17·8141	12·0017
10	0	32·3100	29·5948	26·8327	25·3970	23·8974	20·6099	16·7925
	10	33·2789	30·7533	28·2463	26·9770	25·6833	23·0019	20·2902
	20	34·2138	31·8597	29·5768	28·4494	27·3264	25·1149	23·1373
	−20	36·3402	32·2405	27·7181	25·2450	22·5745	16·2094	3·7922
	−10	37·1218	33·2252	29·0202	26·7805	24·4284	19·2458	12·7009
10^2	0	37·8846	34·1767	30·2565	28·2180	26·1282	21·7966	17·2519
	10	38·6298	35·0979	31·4354	29·5726	27·7040	24·0256	20·6487
	20	39·3585	35·9912	32·5634	30·8560	29·1774	26·0220	23·4398
	−20	38·3623	33·5649	28·5246	25·8553	23·0267	16·4488	4·0934
	−10	39·0951	34·5050	29·7857	27·3511	24·8416	19·4419	12·7840
10^{20}	0	39·8123	35·4159	30·9865	28·7555	26·5107	21·9661	17·3093
	10	40·5146	36·2999	32·1342	30·0822	28·0618	24·1770	20·6950
	20	41·2028	37·1591	33·2348	31·3416	29·5148	26·1603	23·4799

TABLE 10

Values of the frequency parameter Ω of orthotropic circular plates of linearly varying thickness in fundamental mode of vibrations for $\nu_\theta = 0{\cdot}3$, $E_\theta/E_r = 0{\cdot}75$, $D_{k0} = 1{\cdot}4$ and $n = 2$

K_ϕ	$\bar{N}/\alpha$	−0·5	−0·3	−0·1	0·0	0·1	0·3	0·5
	−20	25·2526	20·2284	13·7140	8·8657	–	–	–
	−10	29·0118	25·1565	20·8943	18·5015	15·8079	8·1530	–
0	0	32·3287	29·2594	26·1706	24·6163	23·0534	19·8922	16·6551
	10	35·3294	32·8490	30·5468	29·4888	28·5133	26·9009	25·9734
	20	38·0896	36·0797	34·3689	33·6629	33·0838	32·4179	32·6638
	−20	29·8320	25·9011	21·2481	18·3270	14·6821	–	–
	−10	33·1833	30·0636	26·6743	24·7483	22·6097	17·2198	7·4488
10	0	36·2095	33·6945	31·1423	29·7836	28·3607	25·1985	21·3978
	10	38·9888	36·9546	35·0260	34·0606	33·1019	31·1694	29·2774
	20	41·5724	39·9374	38·5062	37·8419	37·2273	36·1485	35·4174
	−20	36·6208	31·6689	25·8017	22·3255	18·2232	–	–
	−10	39·7248	35·5232	30·8286	28·2450	25·4506	18·8758	8·5510
10^2	0	42·5748	38·9620	35·0975	33·0713	30·9810	26·6064	21·9529
	10	45·2220	42·0922	38·8664	37·2411	35·6251	32·5093	29·7895
	20	47·7029	44·9819	42·2744	40·9614	39·7021	37·4672	35·9248
	−20	38·8111	33·1008	26·6810	22·9990	18·7499	3·1412	–
	−10	41·9198	36·9474	31·6821	28·8803	25·9166	19·1266	8·6754
10^{20}	0	44·7846	40·3931	35·9489	33·7004	31·4355	26·8209	22·0224
	10	47·4526	43·5380	39·7259	37·8756	36·0821	32·7177	29·8561
	20	49·9580	46·4467	43·1471	41·6065	40·1671	37·6771	35·9927

The frequency parameter Ω is found to increase with the increase in E_θ/E_r and also with that of $\bar{N}$ similar to the axisymmetric case. But the rate of increase of frequency parameter here is found to be higher. Tables (10–12) and Figure 7 give the frequency parameter Ω for different values of E_θ/E_r and $\bar{N}$ for $n = 2$ in fundamental mode. The behaviour of Ω

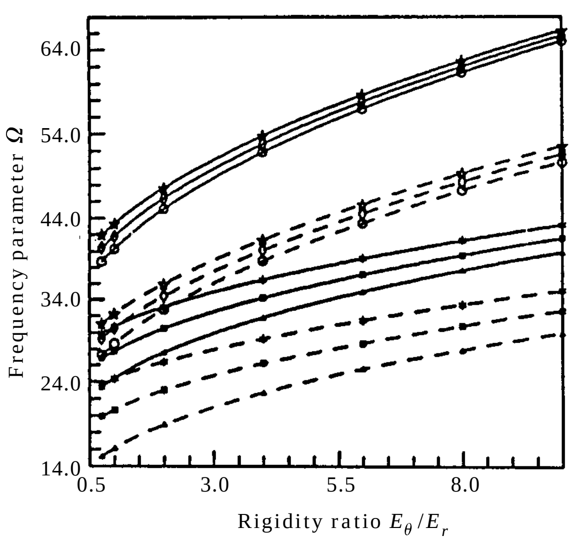

Figure 7. Frequency parameter in antisymmetric ($n = 2$) fundamental mode for SS (– – –) and Cl (——) LVT plates for $\nu_\theta = 0{\cdot}3$. Key as for Figure 5.

TABLE 11

Values of the frequency parameter Ω of orthotropic circular plates of linearly varying thickness in fundamental mode of vibrations for $\nu_\theta = 0{\cdot}3$, $E_\theta/E_r = 1{\cdot}0$, $D_{k0} = 1{\cdot}4$ *and* $n = 2$

K_ϕ	$\bar{N}/\alpha$	−0·5	−0·3	−0·1	0·0	0·1	0·3	0·5
	−20	27·1008	22·0507	15·7042	11·3217	2·9879	–	–
	−10	30·5931	26·6107	22·2376	19·8023	17·0856	9·6706	–
0	0	33·7227	30·4945	27·2469	25·6133	23·9712	20·6519	17·2571
	10	36·5832	33·9354	31·4685	30·3303	29·2767	27·5193	26·4727
	20	39·2337	37·0572	35·1872	34·4063	33·7565	32·9677	33·1266
	−20	31·6690	27·6905	23·0300	20·2076	16·7710	–	–
	−10	34·7788	31·5454	28·0368	26·0865	23·9228	18·4926	9·1767
10	0	37·6242	34·9673	32·2615	30·8481	29·3618	26·0516	22·0982
	10	40·2624	38·0747	35·9832	34·9551	33·9263	31·8449	29·8190
	20	42·7325	40·9404	39·3466	38·6192	37·9358	36·7220	35·8861
	−20	38·6279	33·6121	27·7293	24·2866	20·2934	7·5597	–
	−10	41·4775	37·1511	32·3357	29·6934	26·8456	20·2009	10·2024
10^2	0	44·1263	40·3590	36·3351	34·2259	32·0516	27·5051	22·6714
	10	46·6101	43·3120	39·9143	38·2012	36·4981	33·2127	30·3392
	20	48·9554	46·0610	43·1806	41·7820	40·4400	38·0542	36·3947
	−20	40·9122	35·1087	28·6458	24·9877	20·8279	8·0261	–
	−10	43·7562	38·6326	33·2236	30·3560	27·3264	20·4325	10·3204
10^{20}	0	46·4085	41·8385	37·2148	34·8770	32·5176	27·7142	22·7432
	10	48·9020	44·7973	40·7957	38·8522	36·9622	33·4179	30·4069
	20	51·2611	47·5569	44·0691	42·4384	40·9080	38·2609	36·4628

TABLE 12

Values of the frequency parameter Ω of orthotropic circular plates of linearly varying thickness in fundamental mode of vibrations for $\nu_\theta = 0{\cdot}3$, $E_\theta/E_r = 10{\cdot}0$, $D_{k0} = 1{\cdot}4$ *and* $n = 2$

K_ϕ	$\bar{N}/\alpha$	−0·5	−0·3	−0·1	0·0	0·1	0·3	0·5
	−20	54·9299	47·7228	39·9786	35·7525	31·1211	18·9532	–
	−10	56·4851	49·7544	42·7783	39·1397	35·3486	26·8859	14·6410
0	0	57·9898	51·6893	45·3688	42·1990	39·0290	32·6619	26·2040
	10	59·4482	53·5386	47·7866	45·0020	42·3152	37·3502	33·2965
	20	60·8639	55·3117	50·0589	47·5982	45·3008	41·3586	38·7099
	−20	59·2890	53·0865	46·6335	43·2083	39·5387	30·7948	16·4970
	−10	60·6535	54·7853	48·8152	45·7251	42·4950	35·2654	25·8336
10	0	61·9824	56·4235	50·8868	48·0875	45·2259	39·1493	32·2897
	10	63·2780	58·0067	52·8622	50·3186	47·7724	42·6163	37·4491
	20	64·5475	59·5385	54·7566	52·4752	50·1649	45·7686	41·8324
	−20	67·9791	60·7264	52·8363	48·6126	44·0563	33·6650	18·3884
	−10	69·0749	62·1067	54·6516	50·7426	46·6082	37·6873	26·9626
10^2	0	70·1513	63·4519	56·4000	52·7738	49·0071	41·2592	33·1341
	10	71·2092	64·7652	58·0878	54·7180	51·2756	44·4948	38·1393
	20	72·2495	66·0486	59·7205	56·5845	53·4314	47·4677	42·4253
	−20	71·5178	63·0680	54·2733	49·6696	44·8521	34·0619	18·6055
	−10	72·5489	64·3876	56·0341	51·7477	47·3536	38·0340	27·1004
10^{20}	0	73·5636	65·6771	57·7334	53·7336	49·7102	41·5696	33·2406
	10	74·5627	66·9383	59·3767	55·6375	51·9425	44·7777	38·2284
	20	75·5468	68·1727	60·9689	57·4680	54·0669	47·7288	42·5033

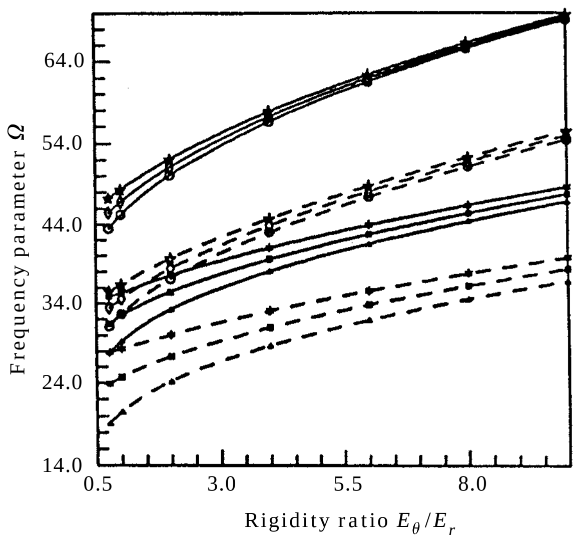

Figure 8. Frequency parameter in axisymmetric second mode for SS (– – –) and Cl (——) LVT plates for $\nu_\theta = 0{\cdot}3$. Key as for Figure 5.

with E_θ/E_r and $\bar{N}$ is similar to those of $n = 0$ and $n = 1$, except for the fact that the effect of $\bar{N}$ is less pronounced. This shows that the effect of $\bar{N}$ decreases with the increasing order of nodal diameter. Figures (8–10) present the behaviour of Ω in the second mode corresponding to $n = 0$, 1 and 2, respectively. Although Ω is found to increase with increasing values of E_θ/E_r and of $\bar{N}$, their effect is found to be decreasing with the increase in the nodal diameter. A similar behaviour is seen in the case of the third mode given in Figures (11–13) corresponding to $n = 0$, 1 and 2.

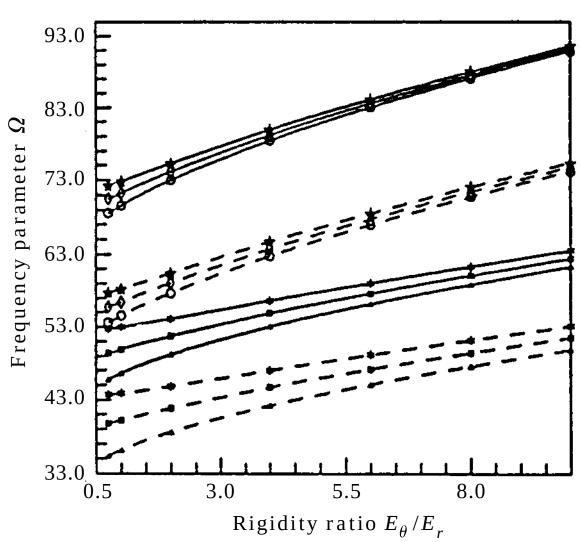

Figure 9. Frequency parameter in antisymmetric ($n = 1$) second mode for SS (– – –) and Cl (——) LVT plates for $\nu_\theta = 0{\cdot}3$. Key as for Figure 5.

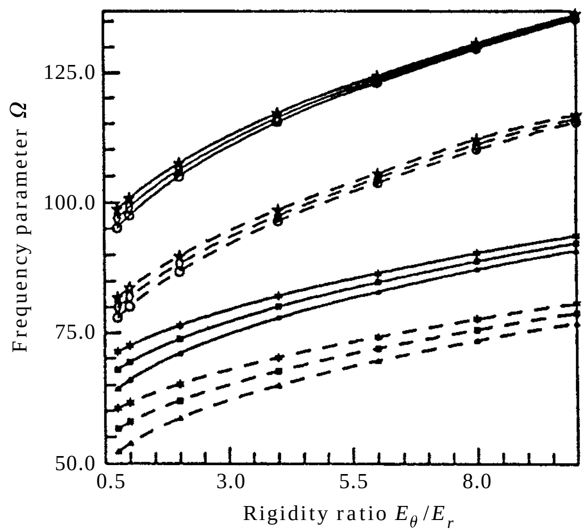

Figure 10. Frequency parameter in antisymmetric ($n = 2$) second mode for SS (– – –) and Cl (——) LVT plates for $\nu_\theta = 0{\cdot}3$. Key as for Figure 5.

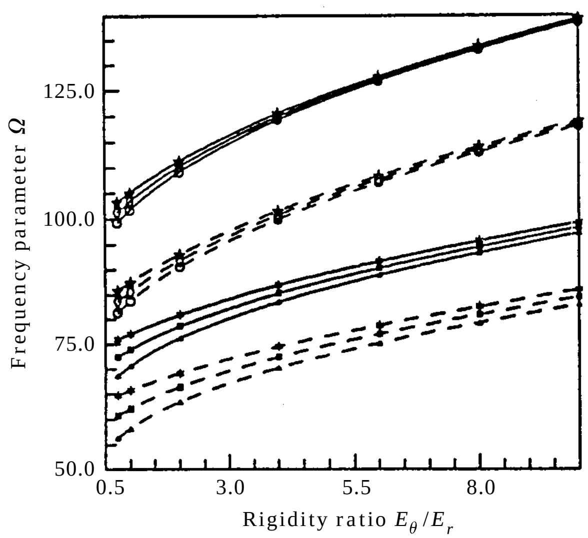

Figure 11. Frequency parameter in axisymmetric third mode for SS (– – –) and Cl (——) LVT plates for $\nu_\theta = 0{\cdot}3$. Key as for Figure 5.

TABLE 13

Comparison of critical buckling load parameter N_{cr} of isotropic plates with those obtained by f.e.m. and exact solution

	$n = 0$			$n = 1$			$n = 2$		
	f.e.m	exact	present	f.e.m.	exact	present	f.e.m.	exact	present
SS	4·1978	4·1978	4·1978	13·1385	13·1381	13·1381	24·8579	24·8557	24·8557
	29·0495	29·0452	29·0452	47·7966	47·7814	47·7824	69·4554	69·4097	69·4097
	73·5495	73·4768	73·4768	102·2246	102·0823	102·0823	133·9121	133·6001	133·6001
Cl	14·6825	14·6820	14·6820	26·3772	26·3746	26·3746	40·7156	40·7064	40·7064
	49·2394	49·2158	49·2158	70·8974	70·8499	70·8499	95·3910	95·2775	95·2775
	103·7035	103·4995	103·4995	135·3394	135·0207	135·0207	170·0089	169·3954	169·3954

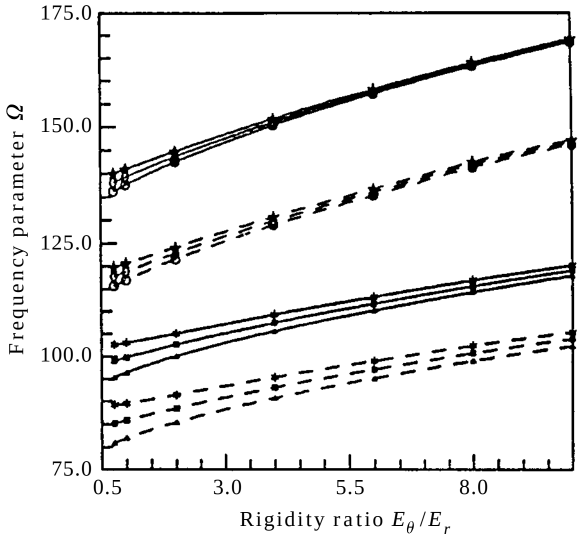

Figure 12. Frequency parameter in antisymmetric ($n = 1$) third mode for SS (– – –) and Cl (——) LVT plates for $\nu_\theta = 0{\cdot}3$. Key as for Figure 5.

The results have been compared in Table 13 with exact solutions given by Vol'mir [9] and those which Pardoen [10] obtained by the finite element method for critical buckling load N_{cr}, for an isotropic plate of uniform thickness for $n = 0$, and 2. Table 14 gives the comparison of results obtained by Bhushan *et al.* [11] using the finite element method for

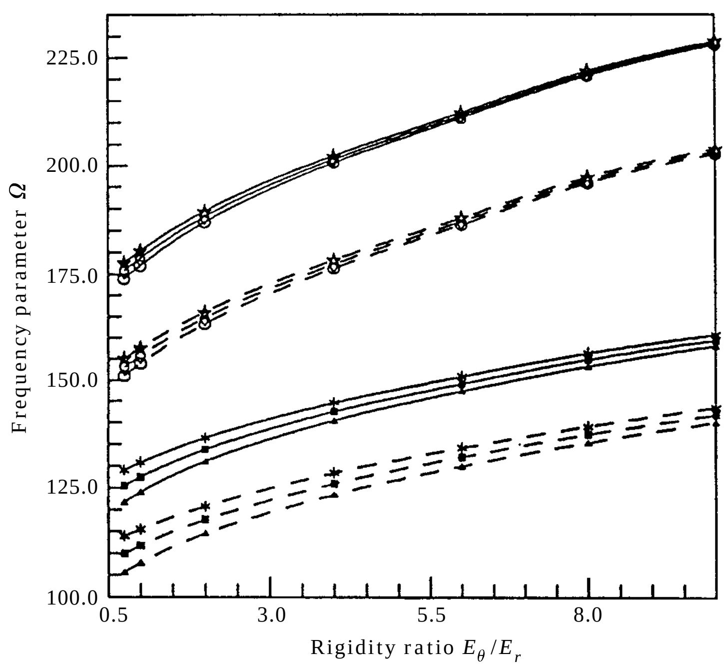

Figure 13. Frequency parameter in antisymmetric ($n = 2$) third mode for SS (– – –) and Cl (——) LVT plates for $\nu_\theta = 0{\cdot}3$. Key as for Figure 5.

orthotropic linearly varying thickness plates. Our results show excellent agreement and much less computational efforts and computer time required as compared to the finite element method. Table 15 presents the comparison with those of Laura *et al*. [19] for isotropic linearly varying thickness plates for different values of the flexibility parameter. The differences in the values here are due to the fact that resultant stress has been taken as constant which is valid only for uniform plates.

The method employed here has the advantage of taking a lesser number of terms in approximating the deflection function than those taken by earlier researchers [6, 19] employing polynomial co-ordinate functions (Table 16).

TABLE 14

Comparison of critical buckling load parameter N_{cr} of tapered orthotropic plates

	f.e.m.		Present (SS)		f.e.m. (Cl)		Present (Cl)	
α/p^2	1	10	1	10	1	10	1	10
−0·5	3·5873	10·4851	3·5873	10·4847	13·5154	32·3417	13·5154	32·3295
−0·3	3·7875	10·0005	3·7875	10·0001	13·9774	30·9003	13·9770	30·8872
0·0	4·1978	9·0693	4·1978	9·0685	14·6824	27·9817	14·6820	27·9670
0·3	4·8014	7·7574	4·8014	7·7556	15·2363	23·5980	15·2357	23·5822
0·5	5·3272	6·7330	5·3270	6·5294	15·2202	19·3163	15·2194	19·3012

TABLE 15

Comparison of critical buckling parameter N_{cr} as a function of the rotational flexibility coefficient and the parameter α in fundamental mode

	Present					From reference [19]				
α/K_ϕ	0	1	10	50	∞	0	1	10	50	∞
−0·3	2·4583	4·4587	7·1460	7·6613	7·8007	2·504	4·561	7·365	7·907	8·054
−0·1	3·5561	5·6863	10·4222	11·7387	12·1143	3·577	5·725	10·522	11·861	12·243
0·0	4·1978	6·3532	12·1725	14·1106	14·6820	4·198	6·353	12·173	14·111	14·682
0·1	4·9070	7·0733	13·9679	16·7010	17·5375	4·879	7·029	13·844	16·535	17·357
0·3	6·5448	8·7090	17·6255	22·5150	24·1521	6·438	8·556	17·196	21·873	23·432

TABLE 16

Comparison of the critical buckling load parameter N_{cr} obtained by using polynomial co-ordinate functions and the present method for $E_\theta/E_r = 10$, $\alpha = -0{\cdot}5$ and $\nu_\theta = 0{\cdot}3$ in fundamental mode

	SS plates			Cl plates		
	$n = 0$	$n = 1$	$n = 2$	$n = 0$	$n = 1$	$n = 2$
Frequency parameter Ω	78·5907	110·6255	183·7395	242·3338	266·8726	351·3451
No. of terms in present method	6	6	8	8	6	10
No. of terms in polynomial co-ordinate function	8	9	10	10	11	13

REFERENCES

1. P. A. A. Laura, G. C. Pardoen, L. E. Luisoni and D. R. Avalos 1981 *Fibre Science and Technology* **15**, 65–77. Transverse vibration of axisymmetric polar orthotropic circular discs elastically restrained against rotation along the edge.
2. P. A. A. Laura, D. R. Avalos and C. D. Galles 1982 *Journal of Sound and Vibration* **82**, 151–156. Vibration and elastic stability of polar orthotropic circular plates of linearly varying thickness.
3. D. G. Gorman 1983 *Earthquake Engineering and structural Dynamics* **11**, 843–855. Vibration of thermally stressed of polar orthotropic annular plates.
4. D. G. Gunaratnam and A. P. Bhattacharya 1989 *Journal of Sound and Vibration* **137**, 383–392. Transverse vibration and stability of polar orthotropic circular plates. High level relationship.
5. U. S. Gupta and R. Lal 1978 *Journal of Sound and Vibration* **58**, 501–507. Buckling and vibration of circular plates of variable thickness.
6. U. S. Gupta, R. Lal and C. P. Verma 1986 *Journal of Sound and Vibration* **104**, 357–369. Buckling and vibrations of polar orthotropic annular plates of variable thickness.
7. U. S. Gupta, R. Lal and R. Sagar 1994 *Indian Journal of Pure and Applied Mathematics* **25**, 1317–1326. Effect of elastic foundation on axisymmetric vibrations of polar orthotropic Mindlin circular plates.
8. U. S. Gupta, R. Lal and S. K. Jain 1991 *Journal of Sound and Vibration* **147**, 423–434. Buckling and vibrations of polar orthotropic circular plates of linearly varying thickness resting on an elastic foundation.
9. A. S. Vol'mir 1966 *Stability of Elastic Systems*. FTD-MT-64-335, WP-AFB, Ohio.
10. G. C. Pardoen 1978 *Computers and Structures* **9**, 89–95. Asymmetric vibration and stability of circular plates.
11. B. Bhushan, G. Singh and G. Venkateswara Rao 1993 *Journal of Computers and Structures* **46**, 421–428. Buckling of tapered orthotropic circular plates using a computationally economic approach.
12. B. Bhushan, G. Singh and G. Venkateswara Rao 1996 *Journal of Computers and Structures* **59**, 21–33. Asymmetric buckling of layered orthotropic circular and annular plates of varying thickness using a computationally economic semi analytic finite element approach.
13. K. A. V. Pandalai and A. Patel, Sharad 1965 *Journal of the Royal Aeronautical Society* **69**, 279–280. Buckling of orthotropic circular plates.
14. E. B. Uthgenant 1965 *Journal of Royal Aeronautical Society* **69**, 279–280. Post buckling of polar orthotropic circular plates.
15. R. K. Jain 1972 *Journal of Sound and Vibration* **23**, 407–414. Vibration of circular plates of variable thickness under in plane force.
16. J. Cheng Chang and A. J. M. Spencer 1989 *Journal of Engineering and Mathematics* **23**, 29–51. Non axisymmetric instability of polar orthotropic annular plates.
17. K. M. Liew, Y. Xiang and S. Kitipornchai 1994 *Journal of Sound and Vibration* **177**, 689–707. Buckling and vibration of annular Mindlin plates with internal concentric ring supports subjected to in plane pressure.
18. C. T. Dyka and J. F. Carney, III 1979 *Journal of Sound and Vibration* **64**, 223–231. Vibration and stability of spinning polar orthotropic annular plates reinforced with edge beams.
19. R. H. Gutierrez, E. Romanelli and P. A. A. Laura 1996 *Journal of Sound and Vibration* **195**, 391–399. Vibration and elastic stability of thin circular plates with variable profile.
20. P. A. A. Laura and R. H. Gutierrez 1991 *Journal of Sound and Vibration* **144**, 149–167. Free vibration of a solid circular plate of linearly varying thickness and attached to a Winkler type foundation.
21. C. S. Kim and S. M. Dickinson 1990 *Journal of Sound and Vibration* **143**, 171–179. The flexural vibration of thin isotropic and polar orthotropic annular and circular plates with elastically restrained peripheries.
22. L. E. Luisoni, P. A. A. Laura and R. Grossi 1977 *Journal of Sound and Vibration* **54**, 62–66. Antisymmetric modes of vibration of a circular plate elastically restrained against rotation and of linearly varying thickness.
23. Y. Narita and A. W. Leissa 1980 *Journal of Sound and Vibration* **70**, 103–116. Transverse vibration of simply supported circular plates having partial elastic constraints.
24. T. Irie, G. Yamada and K. Tanaka 1983 *Journal of Sound and Vibration* **89**, 295–308. Free vibration of a circular plate elastically restrained along some radical segment.

25. S. Azimi 1988 *Journal of Sound and Vibration* **120**, 19–35. Free vibration of circular plates with elastic edge supports using the Receptance method.
26. S. Azimi 1988 *Journal of Sound and Vibration* **120**, 37–52. Free vibration of circular plates with elastic or rigid interior support.
27. S. G. Lekhnitskii 1968 *Anisotropic Plates*. Gordon and Breach Science Publishers, New York.
28. I. H. Shames and C. L. Dyms 1985 *Energy and Finite Element Method in Structural Mechanics*. New York: McGraw-Hill.
29. D. O. Brush and B. O. Almorth 1975 *Buckling of Bars*, *Plates and Shells*. New York: McGraw-Hill.
30. G. K. Ramaiah and V. Kumar 1973 *Journal of Sound and Vibration* **26**, 517–531. Natural frequencies of polar orthotropic annular plates.
31. A. W. Leissa 1969 *Vibration of Plates*, NASA SP **160**.